THE JOURNAL OF BIOLOGICAL CHEMISTRY VOL. 289, NO. 44, pp. 30257–30267, October 31, 2014

Exposure of Phosphatidylserine by Xk-related Protein Family Members during Apoptosis*[S]

Received for publication, May 21, 2014, and in revised form, September 13, 2014 Published, JBC Papers in Press, September 17, 2014, DOI 10.1074/jbc.M114.583419

Jun Suzuki, Eiichi Imanishi, and Shigekazu Nagata[1]

From the Department of Medical Chemistry, Graduate School of Medicine, Kyoto University, Yoshida-Konoe, Sakyo-ku, Kyoto, Kyoto 606-8501, Japan

Background: Xkr8 is essential to scramble phospholipids during apoptosis. The function of other Xkr family members is unknown.
Results: Xkr4, Xkr8, and Xkr9 rescued apoptotic lipid scrambling in *Xkr8*$^{-/-}$ cells.
Conclusion: In the Xkr family, three members support caspase-activated lipid scrambling, and two of them are tissue-specifically expressed.
Significance: Learning the biochemical function of Xkr family members is essential to understand their physiological role.

Apoptotic cells expose phosphatidylserine (PtdSer) on their surface as an "eat me" signal. Mammalian Xk-related (Xkr) protein 8, which is predicted to contain six transmembrane regions, and its *Caenorhabditis elegans* homolog CED-8 promote apoptotic PtdSer exposure. The mouse and human Xkr families consist of eight and nine members, respectively. Here, we found that mouse Xkr family members, with the exception of Xkr2, are localized to the plasma membrane. When *Xkr8*-deficient cells, which do not expose PtdSer during apoptosis, were transformed by Xkr family members, the transformants expressing Xkr4, Xkr8, or Xkr9 responded to apoptotic stimuli by exposing cell surface PtdSer and were efficiently engulfed by macrophages. Like Xkr8, Xkr4 and Xkr9 were found to possess a caspase recognition site in the C-terminal region and to require its direct cleavage by caspases for their function. Site-directed mutagenesis of the amino acid residues conserved among CED-8, Xkr4, Xkr8, and Xkr9 identified several essential residues in the second transmembrane and second cytoplasmic regions. Real time PCR analysis indicated that unlike Xkr8, which is ubiquitously expressed, Xkr4 and Xkr9 expression is tissue-specific.

Phospholipids, which are synthesized at the cytoplasmic side of the endoplasmic reticulum, serve as structural components in cellular membranes. Phospholipids are asymmetrically distributed in the bilayers of membranes other than those of the endoplasmic reticulum (in the endosomal, Golgi, and plasma membranes) (1). In these membranes, amino phospholipids such as phosphatidylserine (PtdSer)[2] and phosphatidylethanolamine are specifically transported from the outer to inner leaflet in an energy-dependent manner to maintain the asymmetrical phospholipid distribution (2). Thus, PtdSer and phosphatidylethanolamine are preferentially located in the cytoplasmic leaflet of these membranes, whereas phosphatidylcholine, sphingomyelin, and glycolipids are located in the extracellular or lumen leaflet (3).

The asymmetry of plasma membranes is disrupted in biological processes such as apoptotic cell death prior to engulfment by macrophages, platelet activation for blood clotting, cell fusion during muscle or bone development, and membrane budding to release enveloped viruses, pyrenocytes, or exosomes (1, 3–6). The process that disrupts asymmetrical phospholipid distribution is thought to be mediated by a "phospholipid scramblase" that nonspecifically scrambles phospholipids between the inner and outer leaflets (3). The identity of this "scramblase" has been elusive (7), but we recently showed that two proteins from different families, transmembrane protein (TMEM) 16F and Xk-related (Xkr) protein 8, support phospholipid scrambling (8, 9).

TMEM16F, which carries eight transmembrane regions, is localized to the plasma membrane and supports phospholipid scrambling in a Ca^{2+}-dependent manner (9). Humans with Scott syndrome, a mild bleeding disorder caused by impaired PtdSer exposure in activated platelets (10), carry a loss-of-function mutation in the *TMEM16F* gene (9, 11), indicating that TMEM16F is important for the phospholipid scrambling in activated platelets. Of the 10 TMEM16 family members, four additional members have been found to support Ca^{2+}-dependent phospholipid scrambling in specific tissues (12).

Xkr8, which is also localized to the plasma membrane, has tentatively been assigned six transmembrane regions (8). Xkr8 has a caspase 3/7 recognition sequence in the C-terminal tail region, and its cleavage by caspases during apoptosis activates the ability of Xkr8 to support phospholipid scrambling. Xkr8 is expressed ubiquitously in various tissues with extremely high levels in the testis. A null mutation of mouse *Xkr8* or the epigenetic repression of the *XKR8* gene expression in human cancer cells blocks PtdSer exposure during apoptosis. *Caenorhabditis elegans* carries one Xkr homolog (CED-8) with a caspase recog-

* This work was supported in part by grants-in-aid for specially promoted research from the Japan Society for the Promotion of Science (to S. N.) and by a grant-in-aid for young scientists (B) from the Japan Society for the Promotion of Science and a research grant from the Takeda Science Foundation (to J. S.).
[S] This article contains supplemental Methods and Figs. S1 and S2.
[1] To whom correspondence should be addressed. Tel.: 81-75-753-9441; Fax: 81-75-753-9446; E-mail: snagata@mfour.med.kyoto-u.ac.jp.
[2] The abbreviations used are: PtdSer, phosphatidylserine; FasL, Fas ligand; IFET, immortalized fetal thymocyte; TMEM, transmembrane protein; XKR, XK-related; CHES, 2-(cyclohexylamino)ethanesulfonic acid; *p*-APMSF, 4-amidinophenylmethanesulfonyl fluoride.

nition sequence in the N-terminal tail, and its cleavage by CED-3 (caspase in *C. elegans*) causes PtdSer to be exposed on the surface of the dying cell during programmed cell death (8, 13).

The human and mouse *Xkr* families consist of nine and eight members, respectively, and mutations or variations in the gene of Xkr members are associated to human diseases (14–16). However, the biochemical function and tissue distribution of Xkr family members are not well understood. In this study, we investigated the PtdSer exposure by Xkr members and found that Xkr4 and Xkr9 could tissue-specifically support the apoptotic PtdSer exposure.

EXPERIMENTAL PROCEDURES

Cell Lines, Recombinant Proteins, Antibodies, and Materials—Human PLB-985 cells (17) were grown in RPMI 1640 medium containing 10% FCS and 50 μM β-mercaptoethanol. Mouse *Xkr8*$^{-/-}$ immortalized fetal thymocytes (IFETs) expressing mouse Fas (IFET-Fas) as described previously (8) were grown in DMEM supplemented with 10% FCS, 1× non-essential amino acids (Invitrogen), GlutaMAX™ (Invitrogen), 10 mM Hepes-NaOH buffer (pH 7.4), and 50 μM β-mercaptoethanol. Mouse WR19L cells transformed with mouse Fas (WR-Fas) as described previously (18) were grown in RPMI 1640 medium containing 10% FCS and 50 μM β-mercaptoethanol. Human HEK293T cells and Plat-E cells (19) were grown in DMEM containing 10% FCS. The leucine zipper-tagged human recombinant Fas ligand (FasL) was prepared as described (20). Allophycocyanin-labeled rat anti-mouse CD11b mAb (Mac1, clone M1/70), rabbit anti-activated caspase-3 mAb, and Alexa Fluor 488-labeled goat anti-rabbit IgG antibody were obtained from BD Pharmingen, Cell Signaling Technology (Danvers, MA), and Invitrogen, respectively. Staurosporine was provided by Kyowa Hakko Kirin (Tokyo, Japan).

Xkr cDNAs—The coding sequences for mouse *Xkr1* (GenBank™ accession number NM_201368), *Xkr2* (GenBank accession number NM_ 183319), *Xkr4* (GenBank accession number NM_001011874), *Xkr5* (GenBank accession number NM_001113350), *Xkr6* (GenBank accession number NM_ 173393), *Xkr7* (GenBank accession number NM_001011732), and *Xkr9* (GenBank accession number NM_001011873) and human *XKR9* (GenBank accession number NM_001011720) were prepared by RT-PCR using cDNA from Ba/F3 cells (*Xkr1*), bone marrow (*Xkr2*), brain (*Xkr4*, *Xkr6*, and *Xkr7*), thymus (*Xkr5* and *Xkr9*), or Jurkat cells (*XKR9*). Primers used for RT-PCR were shown in supplemental Methods. We purchased *XKR4* (GenBank accession number NM_052898) cDNA from DNAFORM (Yokohama, Japan); *Xkr8* and *XKR*8 cDNAs were as described previously (8).

To express proteins tagged with GFP or FLAG at the C terminus, cDNAs were inserted between the BamHI and EcoRI sites or at the EcoRI site of pMXs-puro c-GFP (8) or pMXs-puro c-FLAG (9) after being verified by sequencing. *XKR* cDNAs were inserted into the pNEF vector, pEF-BOS vector (21), which contains the SV40 early promoter-driven neomycin resistance gene.

Xkr Transformation and Cellular Localization—Mouse *Xkr8*$^{-/-}$ IFET cells were transformed by infection with ecotropic retrovirus, whereas mouse WR-Fas and human PLB-985 cells were transformed by infection with pantropic retrovirus. In brief, MLV retroviruses carrying *Xkr* cDNAs were produced by transfecting Plat-E cells with the pMX-puro vector, concentrated by centrifugation at 6000 × *g* for 16 h at 4 °C, and used to infect *Xkr8*$^{-/-}$ IFET-Fas cells. The transformants were selected in medium containing 2.0 μg/ml puromycin. To produce the pantropic retrovirus, HEK293T cells were transfected with the pMXs vector, pGP vector for the gag-pol fusion protein (Takara Bio, Shiga, Japan), and pCMV-VSV-G-RSV-Rev vector for the envelope (provided by Dr. H. Miyoshi, Riken, Tsukuba, Japan); virus particles in the culture supernatant were concentrated by centrifugation. In some cases, PLB-985 cells were transfected with linearized pNEF-XKR-FLAG by electroporation using NEPA21 (Nepagene, Chiba, Japan), and transformants were selected in medium containing 2.0 mg/ml geneticin (Invitrogen).

To examine the cellular localization of Xkr, HEK293T cells were transfected with pMXs-puro Xkr-GFP using FuGENE 6 (Promega, Madison, WI), and stable transformants were selected in medium containing 1.0 μg/ml puromycin. For observation by fluorescence microscopy (BioRevo BZ-9000, Keyence, Osaka, Japan), cells grown on glass bottom dishes (AGC Technoglass, Shizuoka, Japan) were observed in PBS containing 2% FCS.

Apoptosis and Engulfment of Apoptotic Cells by Macrophages—To induce apoptosis, 5 × 10^5 IFET-Fas or WR-Fas cells in 0.5 ml of culture medium were treated with 25 units/ml FasL for 120 min or with 10 units/ml FasL for 50 min, respectively. To induce apoptosis in PLB-985 cells, 5 × 10^5 cells in 0.5 ml of culture medium were treated with 10 μM staurosporine for 2–4 h, or 1 × 10^6 cells in 2 ml of PBS were exposed to 2000 J/m^2 UV irradiation (254 nm) in a StrataLinker (Agilent Technologies, Santa Clara, CA) followed by incubation at 37 °C for 3 h in 4 ml of RPMI 1640 medium containing 10% FCS.

The engulfment of apoptotic cells by macrophages was assayed as described previously (22). In brief, PLB-985 cells were exposed to UV irradiation to induce apoptosis and labeled with 0.1 μg/ml pHrodo™ succinimidyl ester (pHrodo, Invitrogen) to monitor the engulfment. Thioglycollate-elicited peritoneal macrophages prepared as described (23) were incubated at 37 °C for 2 h with the pHrodo-labeled apoptotic cells. The cells were suspended in 20 mM CHES-NaOH buffer (pH 9.0) containing 150 mM NaCl, 2% FCS, and 0.67 μg/ml allophycocyanin-labeled rat anti-mouse Mac1 and analyzed by flow cytometry using a FACSAria. In some cases, 5 × 10^4 macrophages cultured in an 8-well Lab-Tek II chambered cover glass (Nalge Nunc International, Penfield, NY) coated with fibronectin were incubated at 37 °C for 120 min with 3.0 × 10^5 pHrodo-labeled apoptotic cells in 0.3 ml of DMEM containing 10% FCS. The cells were then washed with PBS, suspended in Hanks' balanced salt solution containing 2% FCS, and observed by confocal microscopy (Olympus FV1000).

Western Blotting—Cells were lysed at 4 °C for 1 h in ComplexioLyte48 (Logopharm, Freiburg, Germany) with a protease inhibitor mixture (cOmplete Mini, Roche Applied Science). Insoluble materials were removed by centrifugation at 20,000 × *g* for 15 min after which the lysates were mixed with a ¼ volume of 5× SDS sample buffer (200 mM Tris-HCl (pH 6.8), 10% SDS,

25% glycerol, 5% β-mercaptoethanol, and 0.05% bromophenol blue), incubated overnight at room temperature, separated by SDS-PAGE on a 10–20% gradient gel (Bio Craft, Tokyo, Japan), and transferred to a PVDF membrane (Millipore, Billerica, MA). The membranes were probed with 10,000-fold-diluted mouse anti-FLAG mAb conjugated with HRP (clone M2, Sigma-Aldrich) or with 10,000-fold-diluted mouse anti-GFP mAb (clone JL8, Takara Bio) followed by incubation with 10,000-fold-diluted HRP-conjugated goat anti-mouse Igs (Dako, Carpinteria, CA) using the Can Get Signal system (Toyobo, Osaka, Japan). Peroxidase activity was detected by the Western Lightning® ECL system (PerkinElmer Life Sciences).

Preparation of Membrane Fractions and Treatment with Recombinant Caspases—Membrane fractions were prepared from WR-Fas transformants expressing Xkr-GFP as described previously (24). Briefly, 4×10^8 cells were washed with PBS, pelleted, and stored at −80 °C. The frozen cells were suspended in 6 ml of 10 mM Tris-HCl buffer (pH 7.5) containing 1 mM 4-amidinophenylmethanesulfonyl fluoride (*p*-APMSF), homogenized with a Dounce homogenizer, and mixed with 6 ml of 10 mM Tris-HCl buffer (pH 7.5) containing 0.5 M sucrose, 0.1 M KCl, 10 mM $MgCl_2$, 2 mM $CaCl_2$, and 1 mM *p*-APMSF. Nuclei and mitochondria were removed by sequential centrifugations at 4 °C at 600 × *g* for 10 min and at 8000 × *g* for 10 min. Membrane fractions obtained by centrifugation at 150,000 × *g* for 1 h at 4 °C were solubilized in 350 μl of ComplexioLyte48 at 4 °C for 3 h. Insoluble materials were removed by centrifugation at 20,000 × *g* for 15 min after which the lysates (about 15 μg of protein) were incubated at 37 °C for 1 h with 1.6 units (for Xkr4-GFP) or 0.16 unit (for Xkr9-GFP) of various recombinant human caspases (BioVision, San Francisco, CA) in 50 μl of 50 mM Hepes-NaOH buffer (pH 7.4) containing 50 mM NaCl, 5% glycerol, 5 mM DTT, 10 mM EDTA, 0.1 μM *p*-APMSF, and 0.1% CHAPS. After adding a ¼ volume of 5× SDS sample buffer, the reaction mixture was boiled for 5 min, separated by electrophoresis on a 10–20% gradient gel, and analyzed by blotting with anti-GFP mAb.

Purification of Human XKR8 and Assignment of Its N Terminus—PLB-985 transformants (4.8×10^9 cells) expressing XKR8-FLAG collected from 4.8 liters of culture were washed with PBS, pelleted by centrifugation, and stored at −80 °C. The frozen cells were suspended in 144 ml of 20 mM Tris-HCl buffer (pH 7.5) containing 5 mM EDTA, 5 mM EGTA, and a mixture of protease inhibitors (1 mM pepstatin, 1 mM leupeptin, and 1 mM *p*-APMSF); homogenized with a Dounce homogenizer; and mixed with 62 ml of 20 mM Tris-HCl (pH 7.5) buffer containing 833.3 mM sucrose, 5 mM EGTA, 5 mM EDTA, and a mixture of protease inhibitors. Nuclei and mitochondria were removed at 4 °C by sequential centrifugations at 800 × *g* for 10 min and at 8000 × *g* for 10 min. After the supernatant was centrifuged at 100,000 × *g* for 1 h, the membrane fraction in the precipitate was resuspended in 10 ml of 50 mM Tris-HCl buffer (pH 7.5) containing 150 mM NaCl, 5 mM EGTA, 5 mM EDTA, 1% Triton X-100, and a mixture of protease inhibitors; homogenized by passing it through a 20-gauge needle five times; and dissolved by slow rotation at 4 °C for 2.5 h. After insoluble materials were removed by centrifugation at 100,000 × *g* for 1 h, the supernatant (24 μg of protein) was mixed with 100 μl (bed volume) of FLAG M2-agarose at 4 °C overnight. After washing with 50 mM Tris-HCl buffer (pH 7.5) containing 150 mM NaCl, 5 mM EGTA, 5 mM EDTA, and 1% Triton X-100, proteins bound to the agarose beads were eluted with 200 μl of 50 mM Tris-HCl buffer (pH 7.5) containing 150 mM NaCl, 5 mM EGTA, 5 mM EDTA, 0.1% Triton X-100, 160 ng/μl FLAG peptide (Sigma-Aldrich), and 1 mM *p*-APMSF; this was repeated three times. The eluates were pooled, concentrated to 40 μl using a Microcon YM100 (Amicon, Millipore), and separated by 10–20% SDS-PAGE in which the cathode buffer was supplemented by 1 mM sodium thioglycollate. The proteins were transferred to a PVDF membrane (pore size, 0.2 μm; Millipore) and stained with Coomassie Brilliant Blue. The N-terminal amino acid sequence of the 36-kDa XKR8-FLAG was determined by Edman degradation as a custom service at APRO Life Science Institute (Naruto, Tokushima, Japan).

RESULTS

Cellular Localization of Xkr Family Members—The Xkr family consists of eight members in mice and nine members in humans; XKR3 does not have a counterpart in mice (25). To examine cellular localization, each of the eight Xkr members was fused at the C terminus to GFP, placed under control of the mouse retrovirus promoter long terminal repeat, and stably expressed in human HEK293T cells. Because mouse retrovirus long terminal repeat has weak promoter activity in human cells (21), we thought that this exogenously introduced protein might not form artificial inclusion bodies. In fact, with the exception of Xkr2, all of the Xkr family members localized to the plasma membrane in stable transformants of HEK293T cells (Fig. 1*A*).

PtdSer Exposure by Xkr Family Members—We showed previously that mouse *Xkr8*$^{-/-}$ IFETs, *Xkr8*$^{-/-}$ embryonic fibroblasts, and human PLB-985 and Raji cells in which *XKR8* expression is epigenetically down-regulated do not expose PtdSer in response to apoptotic stimuli (8). To examine the ability of Xkr family members to expose PtdSer, we transformed *Xkr8*$^{-/-}$ IFETs expressing mouse Fas (IFET-Fas) with GFP-fused Xkr family members. Flow cytometry analysis for GFP showed similar expression levels of each fusion protein (Fig. 1*B*). When the transformants were treated with human FasL, Xkr4, Xkr8, and Xkr9, but not other family members, were able to rescue the FasL-induced PtdSer exposure in *Xkr8*$^{-/-}$ IFET-Fas cells (Fig. 1*B*). Similar results were obtained when human PLB-985 transformants expressing Xkr family members were treated with staurosporine, indicating the general ability of Xkr4, Xkr8, and Xkr9 to support apoptotic PtdSer exposure (supplemental Fig. S1).

Members of the human XKR family have 65–96% amino acid sequence identity with their mouse counterparts. When human XKR family members were introduced into PLB-985 cells, transformants expressing XKR4, XKR8, or XKR9 exposed PtdSer in response to UV irradiation. The PtdSer exposure was strongest in transformants expressing XKR8 (Fig. 2*A*). Expressing XKR4, XKR8, or XKR9 in PLB-985 cells had little effect on the UV-induced activation of caspase 3 (Fig. 2*A*), indicating that Xkr4 and Xkr9, like Xkr8, function downstream of the caspases to expose PtdSer. PtdSer exposed on the surface of

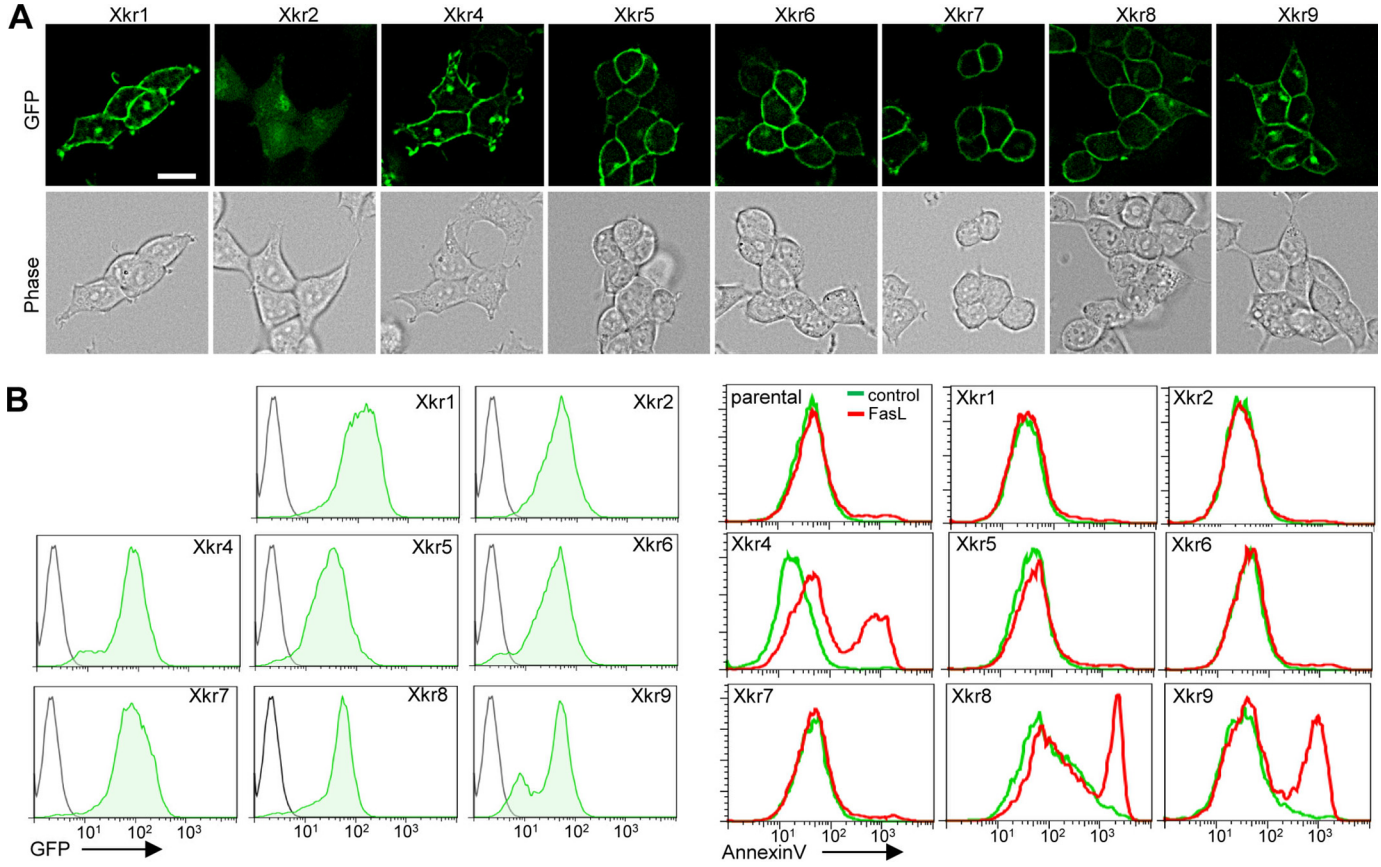

FIGURE 1. **Apoptotic PtdSer exposure by Xkr family members.** *A*, cellular localization of Xkr family members. HEK293T cells were transfected with a pMXs vector encoding the indicated GFP-fused mouse Xkr members, and stable transformants were generated. Cells were observed by fluorescence microscopy for GFP. Phase-contrast images are shown. *Scale bar*, 20 μm. *B*, apoptotic PtdSer exposure by Xkr family members in mouse IFETs. *Xkr8*$^{-/-}$ IFET-Fas cells transformed with the indicated GFP-fused Xkr members were treated with FasL and stained with Cy5-labeled Annexin V. *Left panels*, FACS profiles for GFP (*green*) for each transformant and for the parental cells (*black*). *Right panels*, Annexin V staining profiles for parental *Xkr8*$^{-/-}$ IFET-Fas and for each transformant with (*red*) or without (*green*) FasL treatment.

apoptotic cells serves as an "eat me" signal for macrophages (26, 27). Accordingly, apoptotic UV-treated parental PLB-985 cells, which did not expose PtdSer, were not engulfed by mouse thioglycollate-elicited peritoneal macrophages. However, the PLB-985 cells transformed with XKR4, XKR8, or XKR9 were efficiently engulfed (Fig. 2*B*), confirming that the PtdSer exposed by Xkr family members served as an effective eat me signal.

Caspase Cleavage Sites in Xkr Members—Xkr8 carries a C-terminal caspase 3 recognition site (DQVDG in XKR8 and DLVDG in Xkr8) (Fig. 3) that must be cleaved by caspase 3 or 7 to allow Xkr8 to promote PtdSer exposure (8). To determine whether Xkr4 and Xkr9 could also be cleaved by caspases, mouse WR19L cells expressing mouse Fas (WR-Fas) were transformed with Xkr4-GFP or Xkr9-GFP. The cell membrane fractions were prepared from them, solubilized with the lysis buffer ComplexioLytes-48, and treated with a set of human recombinant caspases (caspases 1–10). As shown in Fig. 4, *B* and *C*, caspases 3, 6, and 7, but not other caspases, cleaved the 95-kDa Xkr4-GFP into a 38-kDa fragment and the 55-kDa Xkr9-GFP into a 27-kDa fragment. These results suggested that Xkr4 was cleaved at a site about 80 amino acids away from its C terminus, whereas the cleavage site of Xkr9 was closer to the C terminus. Both human and mouse Xkr4 and Xkr9 were found to contain phylogenetically well conserved caspase recognition sequences in the C-terminal tail region (AERDG for Xkr4 and DETDG for Xkr9) (Fig. 3 and supplemental Fig. S2). To confirm that Xkr4 and Xkr9 could be cleaved by caspases at AERDG at positions 561–564 of Xkr4-GFP and at DETDG at positions 354–357 of Xkr9-GFP, these sites were mutated to AERAG (Xkr4 1DA) and AETAG (Xkr9 2DA) (Fig. 4*A*). The mutants were expressed in WR-Fas cells, and the membrane fraction was treated with caspase 3, 6, or 7. As shown in Fig. 4, *B* and *C*, these mutants were completely resistant to cleavage by these caspases.

Requirement of Caspase Cleavage for Xkr4- or Xkr9-promoted PtdSer Exposure—To examine whether the cleavage of Xkr4 and Xkr9 was required for their function in exposing PtdSer, WR-Fas transformants expressing Xkr4-GFP, Xkr4 1DA-GFP, Xkr9-GFP, or Xkr9 2DA-GFP were treated with FasL. Western blots of cell lysates indicated that FasL treatment activated caspase 3 in all the transformants, causing wild-type Xkr4-GFP to be cleaved from the 95- to 38-kDa band and Xkr9-GFP to be cleaved from the 55- to 27-kDa band (Fig. 4*D*). However, there was no specific cleavage of Xkr4 or Xkr9 in FasL-treated WR-Fas cells expressing the Xkr4 1DA or Xkr9 2DA mutant, although there was a faint 26-kDa band in some Xkr9 2DA samples.

We next expressed wild-type and caspase-resistant Xkr4 and Xkr9, which were FLAG-tagged at the C terminus, in human PLB-985 cells. The FLAG-tagged, but not GFP-fused, Xkrs

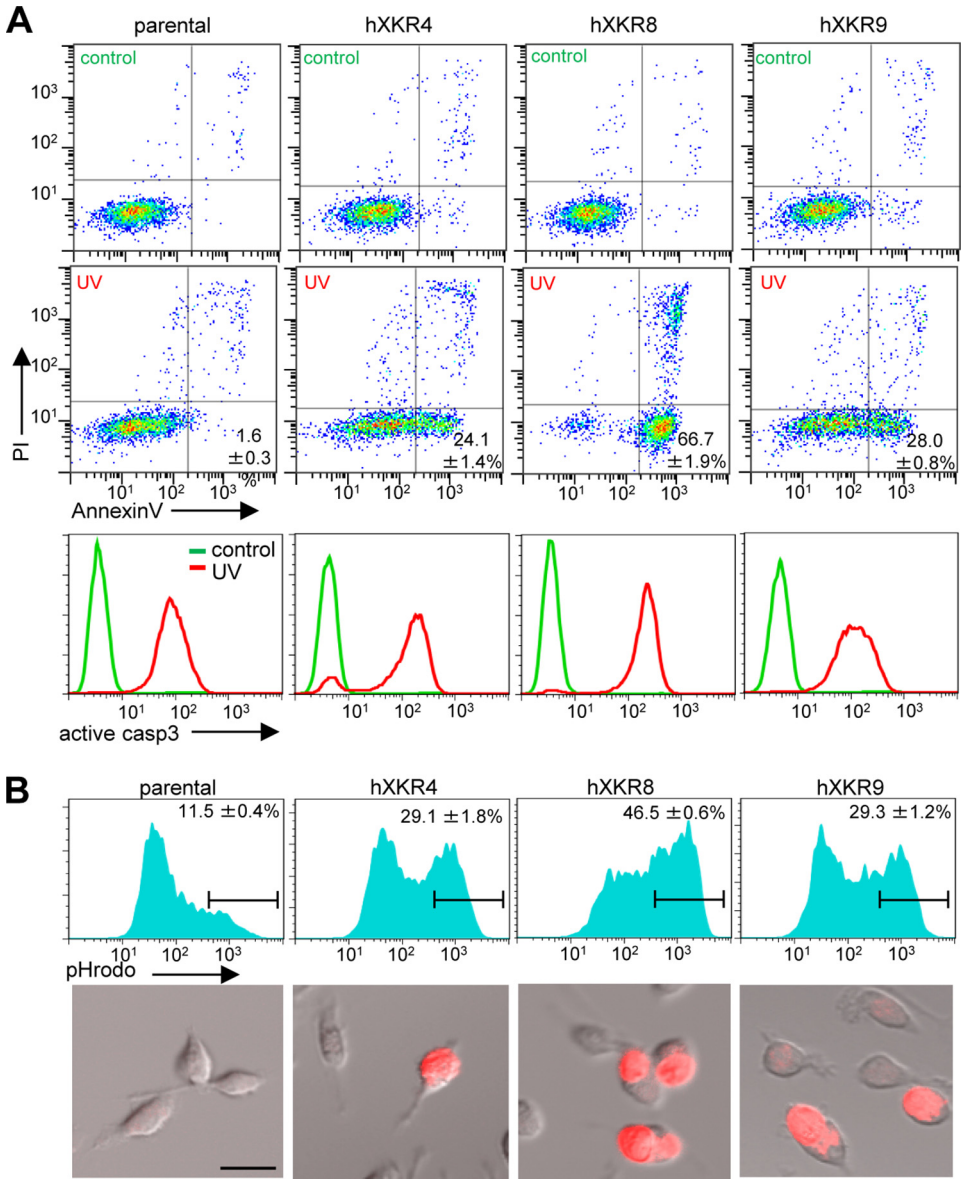

FIGURE 2. **Macrophage engulfment of cells expressing XKRs.** *A*, apoptotic PtdSer exposure by human XKR family members in human PLB-985 cells. UV-exposed or unexposed (control) PLB-985 cells and transformants expressing the indicated human XKR family members were stained with Cy5-Annexin V and propidium iodide (*PI*), and the percentage of Annexin V^+ propidium $iodide^-$ cells was determined. The average values ±S.D. from three independent experiments are shown in the *lower right quadrant*. The *lower panels* show staining profiles for active caspase 3. *B*, engulfment of apoptotic XKR-expressing PLB-985 cells by macrophages. PLB-985 cell transformants expressing the indicated XKR members were exposed to UV irradiation, labeled with pHrodo, and incubated with thioglycollate-elicited mouse peritoneal macrophages; the pHrodo profiles of the $CD11b^+$ population are shown. The average percentage of pHrodo-positive cells ±S.D. is shown for three separate experiments. *Lower panels*, the engulfment of pHrodo-labeled apoptotic cells was observed in a Lab-Tek chamber using confocal microscopy. *Scale bar*, 20 μm.

were used here to confirm that different tags on Xkrs have no adverse effect on the apoptotic PtdSer exposure. As shown in Fig. 4*E*, wild-type and 1DA mutant Xkr4 were expressed at the same level. Staurosporine treatment (10 μM) caused PLB-985 cells expressing wild-type Xkr4 to expose PtdSer, but there was no clear exposure of PtdSer on cells transformed with the Xkr4 1DA mutant (Fig. 4*F*). Wild-type Xkr9 and its 2DA mutant were also expressed at similar levels in PLB-985 cells, although SDS-PAGE indicated a significantly smaller molecular mass (36 kDa) for Xkr9 than the expected molecular weight (43,270) (Fig. 4*E*). Transformants expressing wild-type Xkr9 strongly exposed PtdSer when treated with staurosporine, but PtdSer exposure was severely but not completely blocked by the mutation of the caspase recognition site (Fig. 4*G*). These results indicated that the cleavage by caspases is a system to activate Xkr4 and Xkr9, although the existence of another complementary system can not be ruled out.

Truncation of Xkrs at Caspase Recognition Site—We then truncated Xkr4, Xkr8, and Xkr9 at Asp-564, Asp-354, and Asp-357, respectively (Fig. 4*H*), and introduced them into PLB-985 cells with fused GFP to examine whether they acted as a constitutively active form. The truncated Xkr8 and Xkr9 did not support PtdSer exposure in either growing or apoptotic cells (Fig. 4*I*). Fluorescence microscopy of human 293T cells expressing the truncated Xkr8-GFP and Xkr9-GFP fusion proteins showed that they were present in the cytoplasm, probably in the

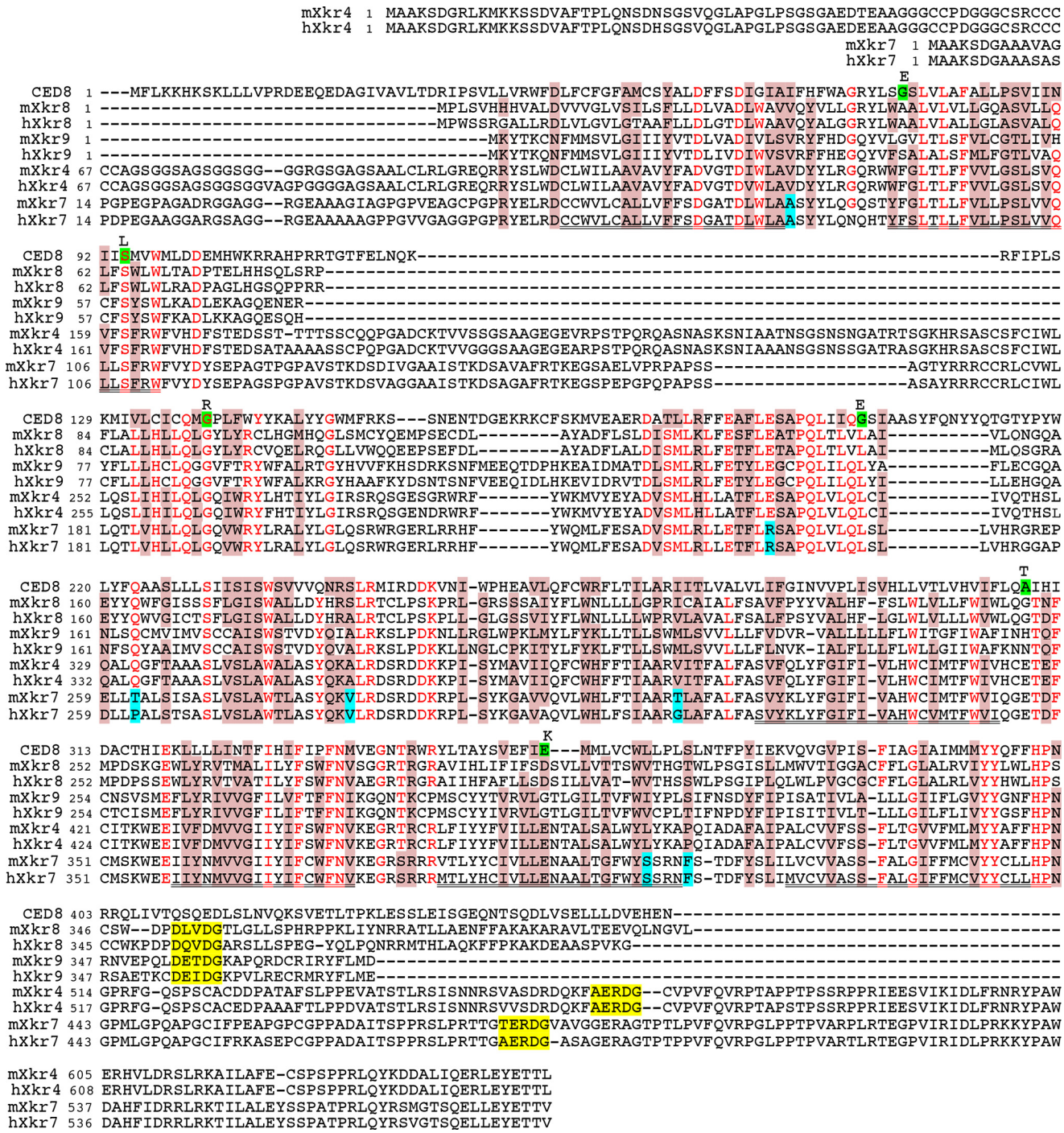

FIGURE 3. **Amino acid sequence alignment of Xkr proteins.** The amino acid sequences of human and mouse Xkr8, Xkr9, Xkr4, and Xkr7 and *C. elegans* CED-8 are shown. Putative transmembrane regions are *underlined*. Identical amino acids conserved in more than seven members are in *red*, and similar amino acids conserved in more than seven members are shaded in *pink*. Similar amino acids are defined as residues belonging to one of the following groups: Ser, Thr, Pro, Ala, and Gly; Asn, Asp, Glu, and Gln; His, Arg, and Lys; Met, Ile, Leu, and Val; or Phe, Tyr, and Trp. Caspase recognition sites are shaded in *yellow*. CED-8 mutations identified by Stanfield and Horvitz (30) are indicated in *green* with the mutated amino acid residue. Xkr7 amino acid residues that differ from the other Xkr proteins are shaded in *blue*.

endoplasmic reticulum (Fig. 4*J*). These results suggested that motifs of dibasic or diaromatic amino acids present downstream of the caspase recognition site of Xkr8 and Xkr9 work as an endoplasmic reticulum export signal(s) (28, 29). Conversely, the truncated Xkr4 efficiently supported the PtdSer exposure in staurosporine-induced apoptotic cells, although it did not support the constitutive PtdSer exposure in living cells (Fig. 4*I*). Different from Xkr8 and Xkr9, Xkr4-GFP was found at the plasma membrane (Fig. 4*J*), suggesting that the 83-amino acid sequence downstream of the caspase recognition site of Xkr4 is essential neither for its localization at the plasma membrane nor for its function to support the apoptotic PtdSer exposure. The result also suggests that in addition to cleavage of Xkr4 another caspase-regulated molecule(s) is involved in the apoptotic scrambling of PtdSer.

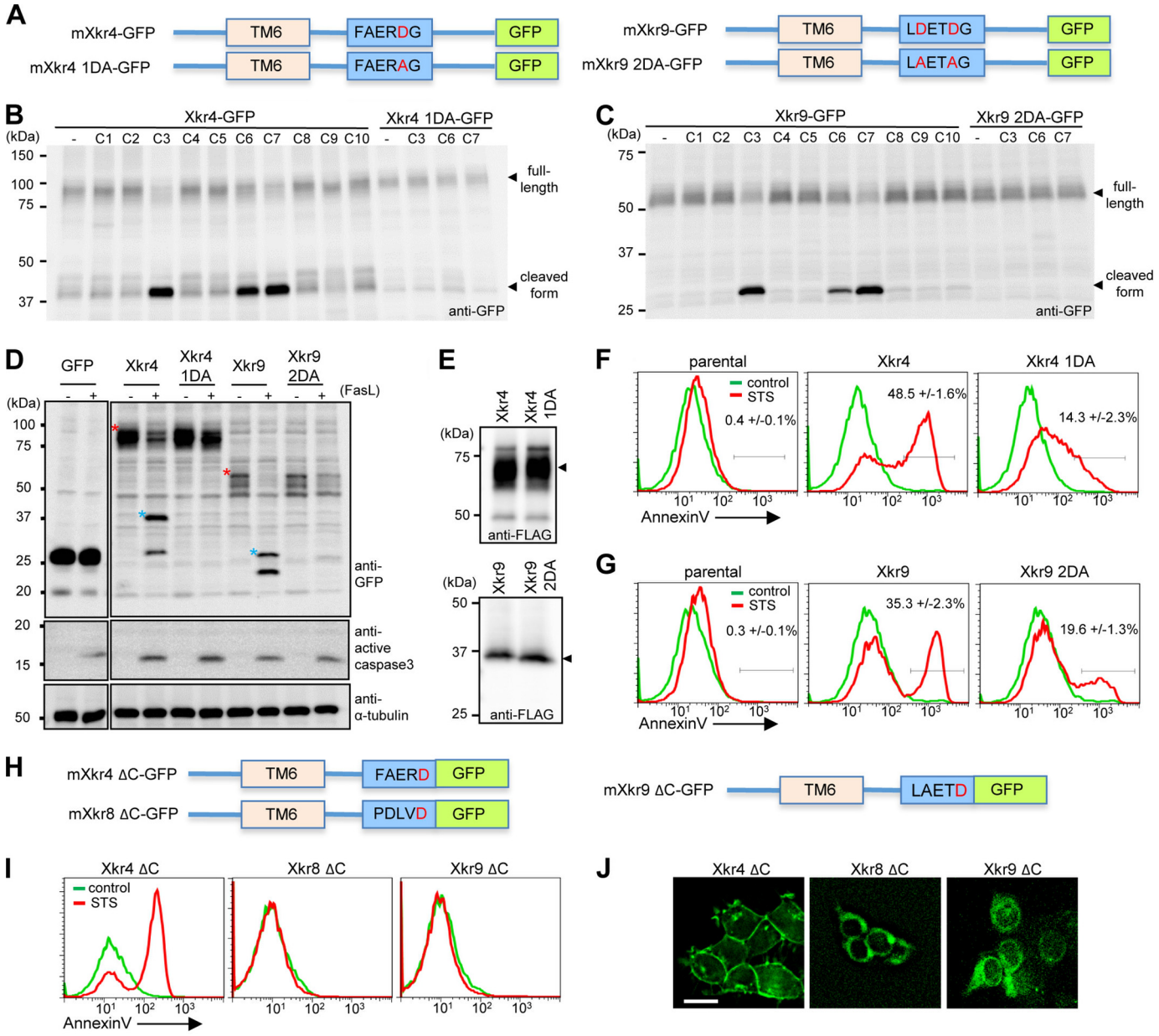

FIGURE 4. **Caspase-mediated Xkr cleavage.** *A*, representations of wild-type (Xkr4 and Xkr9) and caspase-resistant mutant forms (Xkr4 1DA and Xkr9 2DA) fused to GFP. *TM*, transmembrane. *B* and *C*, caspase cleavage of Xkr4 and Xkr9. The solubilized membrane fraction of WR-Fas transformants expressing Xkr4-GFP or Xkr4 1DA-GFP (*B*) or Xkr9-GFP or Xkr9 2DA-GFP (*C*) were incubated for 1 h with recombinant human caspases 1–10 (*C1–C10*) and analyzed by Western blotting with anti-GFP. *Arrowhead*, full-length and cleaved forms of GFP-fused Xkrs. *D*, cleavage of Xkr4 and Xkr9 during apoptosis. WR-Fas transformants expressing GFP, Xkr4-GFP, Xkr4 1DA-GFP, Xkr9-GFP, or Xkr9 2DA-GFP, untreated (−) or treated (+) with FasL for 50 min, were analyzed by Western blotting with anti-GFP, anti-active caspase 3, or anti-α-tubulin. *Red* and *blue asterisks* indicate full-length and cleaved proteins, respectively. *E*, *F*, and *G*, Xkr4 and Xkr9 require cleavage for apoptotic PtdSer exposure. PLB-985 cells were transformed with Xkr4-FLAG, Xkr4 1DA-FLAG, Xkr9-FLAG, or Xkr9 2DA-FLAG and analyzed by Western blotting with an anti-FLAG mAb (*E*). Parental cells and transformants expressing Xkr4-FLAG or Xkr4 1DA-FLAG (*F*) or Xkr9-FLAG or Xkr9 2DA-FLAG (*G*) were treated with staurosporine (*STS*) for 120 (*F*) or 100 min (*G*) and analyzed by flow cytometry with Cy5-labeled Annexin V (*red*), and the percentage of Annexin V-positive cells was determined. The average values and ±S.D. are shown from three separate experiments. The Annexin V staining profiles of untreated cells are shown in *green*. *H*, the structure of the truncation (Δ) mutants of Xkr4, Xkr8, and Xkr9 fused to GFP. *TM*, transmembrane. *I*, PLB-985 transformants expressing Xkr4-ΔC-GFP, Xkr8-ΔC-GFP, or Xkr9-ΔC-GFP were stained with Cy5-labeled Annexin V before (*green*) or after (*red*) treatment with staurosporine for 120 (Xkr4) and for 240 min (Xkr8 and Xkr9). *J*, HEK293T cell transformants expressing Xkr4-ΔC-GFP, Xkr8-ΔC-GFP, or Xkr9-ΔC-GFP were observed by fluorescence microscope. *Scale bar*, 20 μm.

Identification of Indispensable Amino Acid Residues for Xkr8 Function—As mentioned above, the apparent molecular mass of Xkr9 on SDS-PAGE was significantly smaller than the molecular mass calculated from its amino acid composition. We observed this same peculiarity with Xkr8 previously; FLAG-tagged Xkr8 with an expected molecular weight of 46,557 appeared as a 36-kDa protein on SDS-PAGE (8). Because Xkr family members carry a stretch of hydrophobic amino acids near the N terminus (Figs. 3 and 5*A*), this region might function as a signal sequence for transport into the plasma membrane. To examine this possibility, we expressed C-terminally FLAG-tagged XKR8 in PLB-985 cells. The membrane fraction prepared from PLB-985 transformants expressing XKR8 was solubilized with 1% Triton X-100. The FLAG-

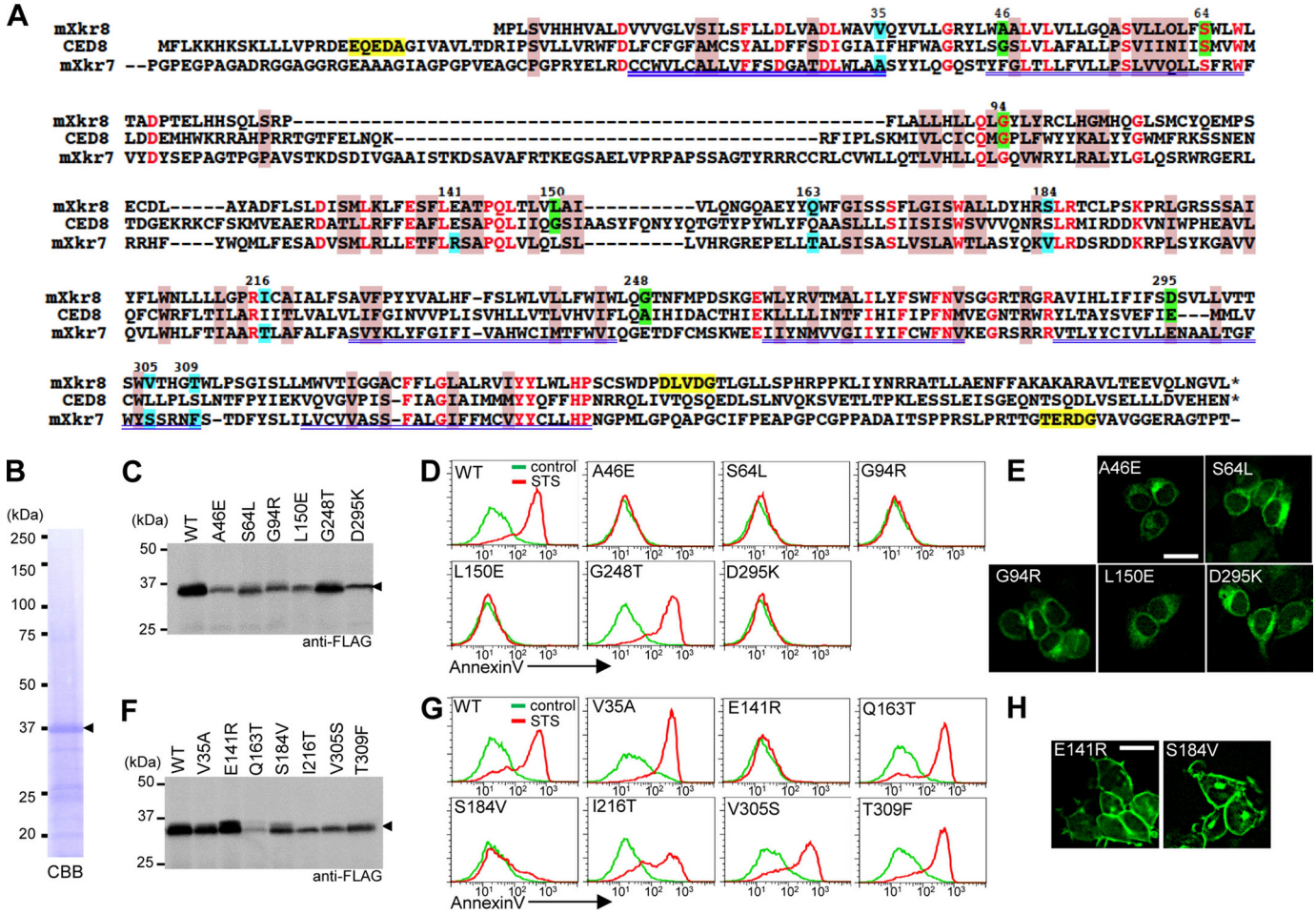

FIGURE 5. **Biochemical analysis of Xkr8.** *A*, amino acid sequence alignment of Xkr8, *C. elegans* CED-8, and Xkr7. The amino acid sequences of Xkr8, *C. elegans* CED-8, and Xkr7 were aligned by introducing several gaps (−) to obtain maximum homology. *Red*, identical amino acids; *pink*, similar amino acids. Transmembrane regions are shown by a *double underline*. Caspase recognition sites are in *yellow*. Amino acid residues of Xkr8 mutated according to CED-8 mutations are in *green*; residues mutated according to Xkr7 are in *blue*. *B*, purification of XKR8. XKR8-FLAG was purified from the membrane fraction of XKR8-FLAG-expressing PLB-985 cells by affinity chromatography. The purified protein was separated by 10–20% SDS-PAGE, transferred to a PVDF membrane, and stained by Coomassie Brilliant Blue (*CBB*). *Arrowhead*, XKR8-FLAG. *C–H*, mutational analysis of Xkr8. PLB-985 cells were transformed with FLAG-tagged wild-type Xkr8 (*WT*); A46E, S64L, G94R, L150E, G248T, and D295K mutants (*C–E*); or V35A, E141R, Q163T, S184V, I216T, V305S, and T309F mutants (*F–H*) and analyzed by Western blotting with an anti-FLAG mAb (*C* and *F*). Transformants were then stained with Cy5-labeled Annexin V before (*control*) or after treatment with staurosporine (*STS*) for 4 h (*D* and *G*). The Xkr8 mutants A46E, S64L, G94R, and L150E (*D*) and E141R and S184V (*G*) that could not support the apoptotic PtdSer exposure were fused to GFP, expressed in HEK293T cells as stable transformants, and observed by fluorescence microscopy (*E* and *H*). *Scale bar*, 20 μm.

tagged XKR8 was affinity-purified and separated by SDS-PAGE (Fig. 5*B*). Edman degradation revealed an N-terminal sequence of PWSSR for the 36-kDa XKR8 (Fig. 3), confirming that there was no processing of XKR8 to a mature protein. Thus, we concluded that the Xkr family proteins probably have six transmembrane regions with N- and C-terminal cytoplasmic termini.

Stanfield and Horvitz (30) previously identified point mutations in CED-8 (G76E, S94L, G139R, G200E, A309T, and E356K) that caused defective CED-8 function *in vivo*. To examine the functional conservation between CED-8 and Xkr8, we mutated the corresponding residues in Xkr8 (A46E, S64L, G94R, L150E, G248T, and D295K) (Fig. 5*A*). These mutants were fused to a FLAG tag at the C terminus and expressed in PLB-985 cells. As shown in Fig. 5*C*, all of the Xkr8 mutants were expressed at a level similar to or slightly reduced from that of wild-type Xkr8. All mutations other than G248T inactivated the ability of Xkr8 to support staurosporine-induced PtdSer exposure in PLB-985 cells (Fig. 5*D*). When the non-functional mutants (A46E, S64L, G94R, L150E, and D295K) were fused to GFP and expressed in HEK293T cells, all the mutants were found in the cytoplasm (Fig. 5*E*), suggesting that these mutations prevented the localization of Xkr8 at the plasma membrane.

In addition to the amino acid sequences in CED-8, Xkr8, XKR8, Xkr9, XKR9, Xkr4, and XKR4 (see Fig. 3), we aligned the sequences in Xkr7 and XKR7; the Xkr7 proteins are highly homologous to Xkr4 with 44.7% identity and have a putative caspase cleavage sequence but were not able to support scramblase activity. We expected to find that important amino acid residues for scrambling were conserved among CED-8, Xkr8, Xkr9, and Xkr4 but not Xkr7. We found seven such amino acid residues: Val-35, Glu-141, Gln-163, Ser-184, Ile-216, Val-305, and Thr-309 (numbering is based on Xkr8) (Fig. 5*A*). We mutated these residues in Xkr8 to the corresponding amino acid sequences in Xkr7 (V35A, E141R, Q163T, S184V, I216T, V305S, and T309F), fused the mutants to FLAG, and expressed them in PLB-985 cells. All of the mutants were expressed at

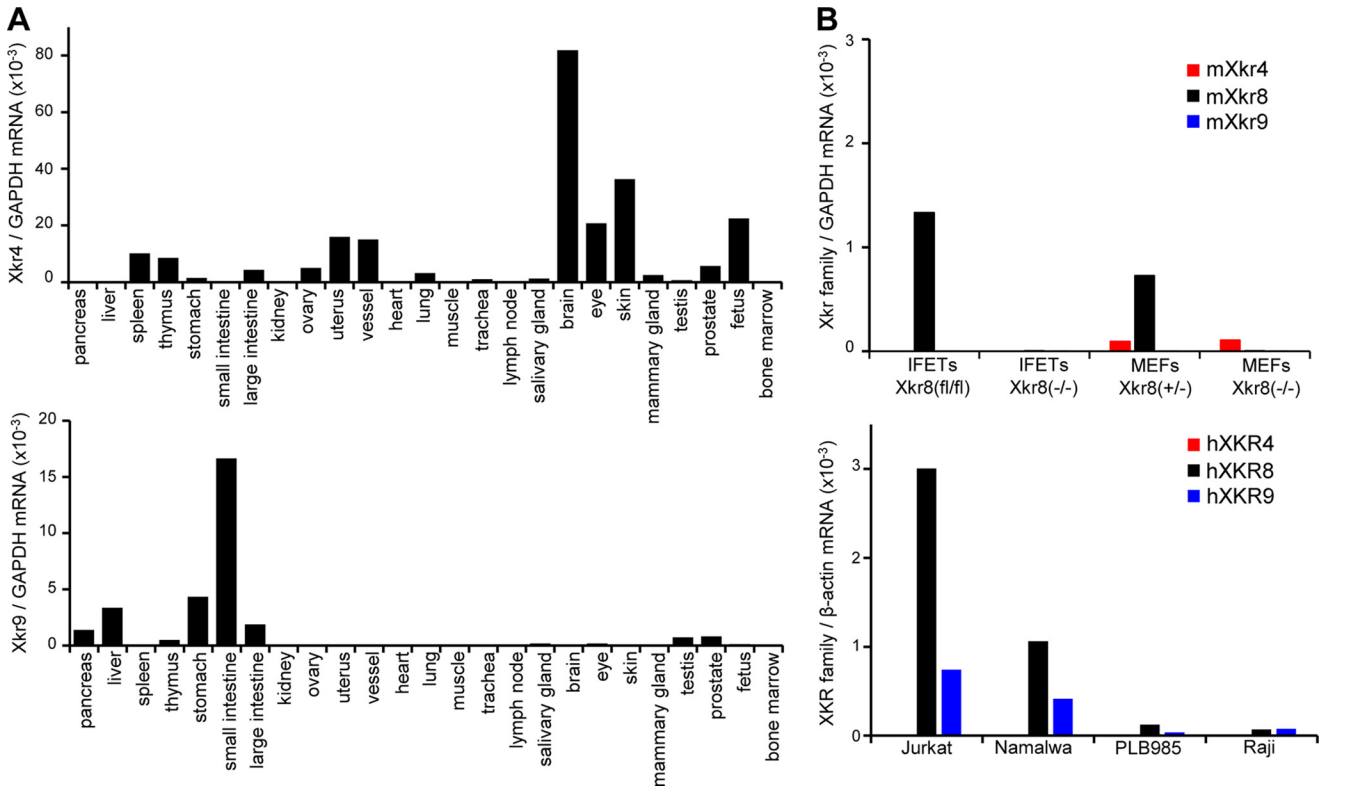

FIGURE 6. **Xkr4 and Xkr9 distribution in mouse tissues and cell lines.** *A*, expression of Xkr4 and Xkr9 mRNA in mouse tissues. Xkr4 and Xkr9 mRNA levels in the indicated mouse tissues were determined by real time RT-PCR and expressed relative to GAPDH mRNA (Xkr4, *upper panel*; Xkr9, *lower panel*). *B*, Xkr4 and Xkr9 expression in mouse IFETs and human cell lines. The levels of Xkr4, Xkr8, and Xkr9 mRNA in the indicated mouse and human cell lines were determined by real time PCR and expressed relative to GAPDH (mouse cell lines) (*upper panel*) or β-actin (human cell lines) (*lower panel*) mRNA. Primers used for real time PCR were described in supplemental Methods.

similar levels (Fig. 5*F*). All mutants except E141R and S184V were able to support PtdSer exposure in response to staurosporine (Fig. 5*G*). The E141R and S184V mutants were localized at plasma membranes (Fig. 5*H*), indicating that the Glu-141 and Ser-184 residues are required for the function of Xkrs and CED-8 to support the apoptotic PtdSer exposure.

Tissue-specific Distribution of Xkr4 and Xkr9—We next analyzed *Xkr4* and *Xkr9* expression in mouse adult tissues using real time RT-PCR. As shown in Fig. 6*A*, *Xkr4* was expressed strongly in the brain and weakly in the spleen, thymus, uterus, blood vessels, and fetus, whereas *Xkr9* was expressed strongly in the small intestines and weakly in the pancreas, liver, stomach, and large intestines. This tissue-specific expression of Xkr4 and Xkr9 contrasts sharply with that of *Xkr8*, which is expressed ubiquitously and at exceptionally high levels in the testis (8).

We reported previously that *Xkr8*$^{-/-}$IFETs and *Xkr8*$^{-/-}$ mouse embryonic fibroblasts do not expose PtdSer in response to apoptotic stimuli (8). Here, real time RT-PCR analysis showed that IFETs and mouse embryonic fibroblasts expressed *Xkr8* but expressed *Xkr4* and *Xkr9* at very low levels (Fig. 6*B*) that appeared to be insufficient to support apoptotic PtdSer exposure. We also observed that human Jurkat and Namalwa cells efficiently expose PtdSer in response to apoptotic stimuli, whereas PLB-985 and Raji cells do not (8). Accordingly, we found that Jurkat and Namalwa cells expressed *XKR8* and *XKR9* but not *XKR4*, whereas PLB-985 and Raji cells expressed none of these Xkr family members (Fig. 6*B*).

DISCUSSION

We and others showed previously that Xkr8/CED-8, predicted to carry six transmembrane regions, is essential to expose PtdSer during apoptosis (8, 13). In the present study, we found that Xkr4 and Xkr9 along with Xkr8 of the mammalian Xkr family support the PtdSer exposure in response to apoptotic stimuli. Xkr4, Xkr8, and Xkr9 possess a caspase recognition site in the C-terminal cytoplasmic tail. Although the caspase recognition sequence is phylogenetically well conserved in each Xkr family member, it differs significantly among Xkr4, Xkr8, and Xkr9, which were targeted differently by caspases; that is, all of these Xkr proteins were efficiently cleaved by caspases 3 and 7, which are furthest downstream in the apoptotic caspase cascade (31), but Xkr4 in particular and Xkr9 were also cleaved by caspase 6.

Unlike Xkr8, which is ubiquitously expressed, we found that Xkr4 and Xkr9 were specifically expressed at high levels in the brain and intestine, respectively. In the brain, a local activation of caspases, in particular caspase 6, has been suggested to contribute to the pruning process of axons, dendrites, and synapses (32–34). It is possible that Xkr4 when activated by caspase 6 induces the exposure of PtdSer on axons, dendrites, and synapses to trigger microglial responses that remodel the neural network. In the small intestine, epithelial cells migrate from the cryptic basement to the villi where they shed off into the lumen via an unknown mechanism (35). An estimated 10^{10} cells are

shed each day from the villi in the human intestine (36). Because caspases are activated in the shedding cells (35), it is tempting to speculate that caspase-activated Xkr9 is responsible for the shedding of aged epithelial cells into the lumen.

The C-terminal portion of Xkr4, Xkr8, or Xkr9 (Ref. 8 and this report) or the N-terminal portion of CED-8 (13) must be cleaved off to activate the phospholipid-scrambling activity. During apoptosis, caspases inactivate many cellular components that are essential for the life of the cell while at the same time activating enzymes (including the caspases themselves) and other factors that execute the cell death program (37). For example, cleavage of the inhibitor of caspase-activated DNase by caspase 3 activates a DNase, caspase-activated DNase, that causes apoptotic DNA fragmentation (38), and the caspase 3-mediated cleavage of Pannexin 1 causes ATP (39) and AMP (40) to be released as "find me" or "calm down" signals to macrophages. The Xkr-mediated cell surface exposure of PtdSer offers another example of activation by caspase cleavage. The mechanism of activation by caspase cleavage differs among proteins; the cleavage of inhibitor of caspase-activated DNase reduces its ability to bind caspase-activated DNase (41, 42), whereas the cleavage of Pannexin 1 removes a C-terminal domain that inhibits its channel activity (43). For Xkr family proteins, the C-terminal tail cleaved off by caspase is very short (only 16 amino acids in Xkr9), and it is unlikely that this region has an inhibitory function in the uncleaved form. When Xkr4 was truncated at the caspase cleavage site, it localized at the plasma membrane but did not function as a constitutively active form, suggesting that it needs another caspase-regulated partner to scramble phospholipids. We recently found that Xkr8 forms multiple oligomers,[3] supporting this notion. Furthermore, although analysis by site-directed mutagenesis indicated that phospholipid scrambling proceeds by similar mechanisms when mediated by Xkr in mammalian cells or by CED-8 in *C. elegans*, CED-8 did not promote apoptotic phospholipid scrambling in mouse cells,[3] which may suggest that Xkr/CED-8 requires a species-specific partner(s) to be functional. Whether Xkr4, Xkr8, or Xkr9 by itself functions as a scramblase or another molecule(s) is necessary could be examined by *in vitro* reconstitution assays applied in the various systems (44–46).

Of the eight members of the mouse Xkr family, all but Xkr2 were found to be localized to plasma membranes, and only three (Xkr4, Xkr8, and Xkr9) facilitated apoptotic PtdSer exposure. Rivera *et al.* (47) recently reported that XK (Xkr1) regulates cell volume by transporting divalent cations. Of the 10-member TMEM16 family, five members function as Ca^{2+}-dependent phospholipid scramblases, whereas two members carry Cl^- channel activity (12, 48, 49). Thus, as in the TMEM16 family, other Xkr family members that are localized to the plasma membrane may act as ion channels. In this regard, it might be interesting to determine whether Xkr7, which carries a caspase recognition site at the C-terminal tail, plays a role as an ion channel for the cell shrinkage during apoptosis.

[3] J. Suzuki and S. Nagata, unpublished observations.

Acknowledgment—We thank M. Fujii for secretarial assistance.

REFERENCES

1. van Meer, G., Voelker, D. R., and Feigenson, G. W. (2008) Membrane lipids: where they are and how they behave. *Nat. Rev. Mol. Cell Biol.* **9,** 112–124
2. Coleman, J. A., Quazi, F., and Molday, R. S. (2013) Mammalian P4-ATPases and ABC transporters and their role in phospholipid transport. *Biochim. Biophys. Acta* **1831,** 555–574
3. Leventis, P. A., and Grinstein, S. (2010) The distribution and function of phosphatidylserine in cellular membranes. *Annu. Rev. Biophys.* **39,** 407–427
4. Yoshida, H., Kawane, K., Koike, M., Mori, Y., Uchiyama, Y., and Nagata, S. (2005) Phosphatidylserine-dependent engulfment by macrophages of nuclei from erythroid precursor cells. *Nature* **437,** 754–758
5. Hanayama, R., and Nagata, S. (2005) Impaired involution of mammary glands in the absence of milk fat globule EGF factor 8. *Proc. Natl. Acad. Sci. U.S.A.* **102,** 16886–16891
6. van Meer, G. (2011) Dynamic transbilayer lipid asymmetry. *Cold Spring Harb. Perspect. Biol.* **3,** a004671
7. Bevers, E. M., and Williamson, P. L. (2010) Phospholipid scramblase: an update. *FEBS Lett.* **584,** 2724–2730
8. Suzuki, J., Denning, D. P., Imanishi, E., Horvitz, H. R., and Nagata, S. (2013) Xk-related protein 8 and CED-8 promote phosphatidylserine exposure in apoptotic cells. *Science* **341,** 403–406
9. Suzuki, J., Umeda, M., Sims, P. J., and Nagata, S. (2010) Calcium-dependent phospholipid scrambling by TMEM16F. *Nature* **468,** 834–838
10. Zwaal, R. F., Comfurius, P., and Bevers, E. M. (2004) Scott syndrome, a bleeding disorder caused by defective scrambling of membrane phospholipids. *Biochim. Biophys. Acta* **1636,** 119–128
11. Castoldi, E., Collins, P. W., Williamson, P. L., and Bevers, E. M. (2011) Compound heterozygosity for 2 novel TMEM16F mutations in a patient with Scott syndrome. *Blood* **117,** 4399–4400
12. Suzuki, J., Fujii, T., Imao, T., Ishihara, K., Kuba, H., and Nagata, S. (2013) Calcium-dependent phospholipid scramblase activity of TMEM16 protein family members. *J. Biol. Chem.* **288,** 13305–13316
13. Chen, Y.-Z., Mapes, J., Lee, E.-S., Skeen-Gaar, R. R., and Xue, D. (2013) Caspase-mediated activation of *Caenorhabditis elegans* CED-8 promotes apoptosis and phosphatidylserine externalization. *Nat. Commun.* **4,** 2726
14. Porto Neto, L. R., Bunch, R. J., Harrison, B. E., and Barendse, W. (2012) Variation in the XKR4 gene was significantly associated with subcutaneous rump fat thickness in indicine and composite cattle. *Anim. Genet.* **43,** 785–789
15. Ho, M., Chelly, J., Carter, N., Danek, A., Crocker, P., and Monaco, A. P. (1994) Isolation of the gene for McLeod syndrome that encodes a novel membrane transport protein. *Cell* **77,** 869–880
16. Alonso-Perez, E., Suarez-Gestal, M., Calaza, M., Ordi-Ros, J., Balada, E., Bijl, M., Papasteriades, C., Carreira, P., Skopouli, F. N., Witte, T., Endreffy, E., Marchini, M., Migliaresi, S., Sebastiani, G. D., Santos, M. J., Suarez, A., Blanco, F. J., Barizzone, N., Pullmann, R., Ruzickova, S., Lauwerys, B. R., Gomez-Reino, J. J., Gonzalez, A., and European Consortium of SLE DNA Collections (2012) Further evidence of subphenotype association with systemic lupus erythematosus susceptibility loci: a European cases only study. *PLoS One* **7,** e45356
17. Tucker, K. A., Lilly, M. B., Heck, L., Jr., and Rado, T. A. (1987) Characterization of a new human diploid myeloid leukemia cell line (PLB-985) with granulocytic and monocytic differentiating capacity. *Blood* **70,** 372–378
18. Watanabe-Fukunaga, R., Brannan, C. I., Copeland, N. G., Jenkins, N. A., and Nagata, S. (1992) Lymphoproliferation disorder in mice explained by defects in Fas antigen that mediates apoptosis. *Nature* **356,** 314–317
19. Morita, S., Kojima, T., and Kitamura, T. (2000) Plat-E: an efficient and stable system for transient packaging of retroviruses. *Gene Ther.* **7,** 1063–1066
20. Shiraishi, T., Suzuyama, K., Okamoto, H., Mineta, T., Tabuchi, K., Nakayama, K., Shimizu, Y., Tohma, J., Ogihara, T., Naba, H., Mochizuki, H., and Nagata, S. (2004) Increased cytotoxicity of soluble Fas ligand by fusing

isoleucine zipper motif. *Biochem. Biophys. Res. Commun.* **322,** 197–202
21. Mizushima, S., and Nagata, S. (1990) pEF-BOS, a powerful mammalian expression vector. *Nucleic Acids Res.* **18,** 5322
22. Toda, S., Hanayama, R., and Nagata, S. (2012) Two-step engulfment of apoptotic cells. *Mol. Cell. Biol.* **32,** 118–125
23. Hanayama, R., Tanaka, M., Miwa, K., Shinohara, A., Iwamatsu, A., and Nagata, S. (2002) Identification of a factor that links apoptotic cells to phagocytes. *Nature* **417,** 182–187
24. Fukunaga, R., Ishizaka-Ikeda, E., and Nagata, S. (1990) Purification and characterization of the receptor for murine granulocyte colony-stimulating factor. *J. Biol. Chem.* **265,** 14008–14015
25. Calenda, G., Peng, J., Redman, C. M., Sha, Q., Wu, X., and Lee, S. (2006) Identification of two new members, XPLAC and XTES, of the XK family. *Gene* **370,** 6–16
26. Nagata, S., Hanayama, R., and Kawane, K. (2010) Autoimmunity and the clearance of dead cells. *Cell* **140,** 619–630
27. Ravichandran, K. S. (2010) Find-me and eat-me signals in apoptotic cell clearance: progress and conundrums. *J. Exp. Med.* **207,** 1807–1817
28. Giraudo, C. G., and Maccioni, H. J. (2003) Endoplasmic reticulum export of glycosyltransferases depends on interaction of a cytoplasmic dibasic motif with Sar1. *Mol. Biol. Cell* **14,** 3753–3766
29. Barlowe, C. (2003) Signals for COPII-dependent export from the ER: what's the ticket out? *Trends Cell Biol.* **13,** 295–300
30. Stanfield, G. M., and Horvitz, H. R. (2000) The ced-8 gene controls the timing of programmed cell deaths in *C. elegans*. *Mol. Cell* **5,** 423–433
31. Taylor, R. C., Cullen, S. P., and Martin, S. J. (2008) Apoptosis: controlled demolition at the cellular level. *Nat. Rev. Mol. Cell Biol.* **9,** 231–241
32. Cusack, C. L., Swahari, V., Hampton Henley, W., Michael Ramsey, J., and Deshmukh, M. (2013) Distinct pathways mediate axon degeneration during apoptosis and axon-specific pruning. *Nat. Commun.* **4,** 1876
33. Nikolaev, A., McLaughlin, T., O'Leary, D. D., and Tessier-Lavigne, M. (2009) APP binds DR6 to trigger axon pruning and neuron death via distinct caspases. *Nature* **457,** 981–989
34. Han, C., Song, Y., Xiao, H., Wang, D., Franc, N. C., Jan, L. Y., and Jan, Y. N. (2014) Epidermal cells are the primary phagocytes in the fragmentation and clearance of degenerating dendrites in *Drosophila*. *Neuron* **81,** 544–560
35. Bullen, T. F., Forrest, S., Campbell, F., Dodson, A. R., Hershman, M. J., Pritchard, D. M., Turner, J. R., Montrose, M. H., and Watson, A. J. (2006) Characterization of epithelial cell shedding from human small intestine. *Lab. Invest.* **86,** 1052–1063
36. Potten, C. S., and Loeffler, M. (1990) Stem cells: attributes, cycles, spirals, pitfalls and uncertainties. Lessons for and from the crypt. *Development* **110,** 1001–1020
37. Crawford, E. D., and Wells, J. A. (2011) Caspase substrates and cellular remodeling. *Annu. Rev. Biochem.* **80,** 1055–1087
38. Nagata, S. (2005) DNA degradation in development and programmed cell death. *Annu. Rev. Immunol.* **23,** 853–875
39. Chekeni, F. B., Elliott, M. R., Sandilos, J. K., Walk, S. F., Kinchen, J. M., Lazarowski, E. R., Armstrong, A. J., Penuela, S., Laird, D. W., Salvesen, G. S., Isakson, B. E., Bayliss, D. A., and Ravichandran, K. S. (2010) Pannexin 1 channels mediate 'find-me' signal release and membrane permeability during apoptosis. *Nature* **467,** 863–867
40. Yamaguchi, H., Maruyama, T., Urade, Y., and Nagata, S. (2014) Immunosuppression via adenosine receptor activation by adenosine monophosphate released from apoptotic cells. *eLife* **3,** e02172
41. McCarty, J. S., Toh, S. Y., and Li, P. (1999) Multiple domains of DFF45 bind synergistically to DFF40: roles of caspase cleavage and sequestration of activator domain of DFF40. *Biochem. Biophys. Res. Commun.* **264,** 181–185
42. Sakahira, H., Enari, M., and Nagata, S. (1998) Cleavage of CAD inhibitor in CAD activation and DNA degradation during apoptosis. *Nature* **391,** 96–99
43. Sandilos, J. K., Chiu, Y.-H., Chekeni, F. B., Armstrong, A. J., Walk, S. F., Ravichandran, K. S., and Bayliss, D. A. (2012) Pannexin 1, an ATP release channel, is activated by caspase cleavage of its pore-associated C-terminal autoinhibitory region. *J. Biol. Chem.* **287,** 11303–11311
44. Malvezzi, M., Chalat, M., Janjusevic, R., Picollo, A., Terashima, H., Menon, A. K., and Accardi, A. (2013) Ca^{2+}-dependent phospholipid scrambling by a reconstituted TMEM16 ion channel. *Nat. Commun.* **4,** 2367
45. Menon, I., Huber, T., Sanyal, S., Banerjee, S., Barré, P., Canis, S., Warren, J. D., Hwa, J., Sakmar, T. P., and Menon, A. K. (2011) Opsin is a phospholipid flippase. *Curr. Biol.* **21,** 149–153
46. Mohammadi, T., van Dam, V., Sijbrandi, R., Vernet, T., Zapun, A., Bouhss, A., Diepeveen-de Bruin, M., Nguyen-Distèche, M., de Kruijff, B., and Breukink, E. (2011) Identification of FtsW as a transporter of lipid-linked cell wall precursors across the membrane. *EMBO J.* **30,** 1425–1432
47. Rivera, A., Kam, S. Y., Ho, M., Romero, J. R., and Lee, S. (2013) Ablation of the Kell/Xk complex alters erythrocyte divalent cation homeostasis. *Blood Cells Mol. Dis.* **50,** 80–85
48. Kunzelmann, K., Nilius, B., Owsianik, G., Schreiber, R., Ousingsawat, J., Sirianant, L., Wanitchakool, P., Bevers, E. M., and Heemskerk, J. W. (2014) Molecular functions of anoctamin 6 (TMEM16F): a chloride channel, cation channel, or phospholipid scramblase? *Pflugers Arch.* **466,** 407–414
49. Pedemonte, N., and Galietta, L. J. (2014) Structure and function of TMEM16 proteins (anoctamins). *Physiol. Rev.* **94,** 419–459